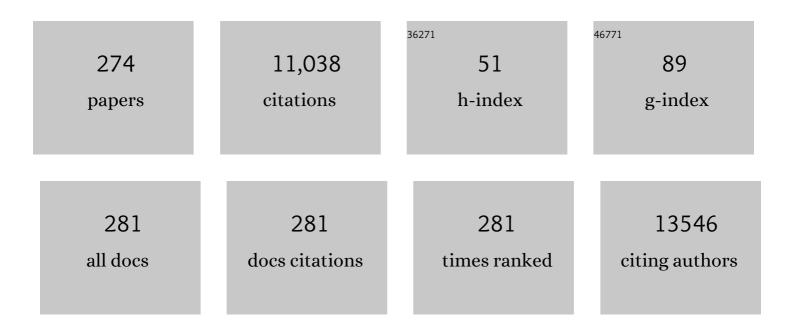
Nam-Joon Cho

List of Publications by Year in descending order

Source: https://exaly.com/author-pdf/770612/publications.pdf Version: 2024-02-01



NAM-LOON CHO

#	Article	IF	CITATIONS
1	Lipid coating technology: A potential solution to address the problem of sticky containers and vanishing drugs. View, 2022, 3, 20200078.	2.7	15
2	Nanoarchitectured air-stable supported lipid bilayer incorporating sucrose–bicelle complex system. Nano Convergence, 2022, 9, 3.	6.3	1
3	Thermodynamic Modeling of Solvent-Assisted Lipid Bilayer Formation Process. Micromachines, 2022, 13, 134.	1.4	5
4	Multivalency-Induced Shape Deformation of Nanoscale Lipid Vesicles: Size-Dependent Membrane Bending Effects. Journal of Physical Chemistry Letters, 2022, 13, 1480-1488.	2.1	5
5	Streamlined Fabrication of Hybrid Lipid Bilayer Membranes on Titanium Oxide Surfaces: A Comparison of One- and Two-Tail SAM Molecules. Nanomaterials, 2022, 12, 1153.	1.9	6
6	Selective Recognition of Phosphatidylinositol Phosphate Receptors by C-Terminal Tail of Mitotic Kinesin-like Protein 2 (MKlp2). Journal of Physical Chemistry B, 2022, 126, 2345-2352.	1.2	3
7	Inkjet-Printed Phospholipid Bilayers on Titanium Oxide Surfaces: Towards Functional Membrane Biointerfaces. Membranes, 2022, 12, 361.	1.4	7
8	Recyclable and Reusable Natural Plantâ€Based Paper for Repeated Digital Printing and Unprinting. Advanced Materials, 2022, 34, e2109367.	11.1	7
9	Microplastics released from food containers can suppress lysosomal activity in mouse macrophages. Journal of Hazardous Materials, 2022, 435, 128980.	6.5	40
10	Unraveling the distinct germination processes of sporopollenin-based pollen grains and spores through morphological analyses upon natural nano-architectonics process. Applied Materials Today, 2022, 27, 101471.	2.3	3
11	Highly substituted decoupled gelatin methacrylamide free of hydrolabile methacrylate impurities: An optimum choice for long-term stability and cytocompatibility. International Journal of Biological Macromolecules, 2021, 167, 479-490.	3.6	10
12	Biomimetic Nanomaterial Strategies for Virus Targeting: Antiviral Therapies and Vaccines. Advanced Functional Materials, 2021, 31, 2008352.	7.8	25
13	Stopping Membrane-Enveloped Viruses with Nanotechnology Strategies: Toward Antiviral Drug Development and Pandemic Preparedness. ACS Nano, 2021, 15, 125-148.	7.3	46
14	Self-Assembly of Solubilized Human Hair Keratins. ACS Biomaterials Science and Engineering, 2021, 7, 83-89.	2.6	7
15	Real-time nanoplasmonic sensing of three-dimensional morphological changes in a supported lipid bilayer and antimicrobial testing applications. Biosensors and Bioelectronics, 2021, 174, 112768.	5.3	13
16	Chemical design principles of next-generation antiviral surface coatings. Chemical Society Reviews, 2021, 50, 9741-9765.	18.7	31
17	Comparing Protein Adsorption onto Alumina and Silica Nanomaterial Surfaces: Clues for Vaccine Adjuvant Development. Langmuir, 2021, 37, 1306-1314.	1.6	14
18	Conformational stability as a quality attribute for the cell therapy raw material human serum albumin. RSC Advances, 2021, 11, 15332-15339.	1.7	4

#	Article	IF	CITATIONS
19	Engineered lipid bicelle nanostructures for membrane-disruptive antibacterial applications. Applied Materials Today, 2021, 22, 100947.	2.3	7
20	Addressing the digital skills gap for future education. Nature Human Behaviour, 2021, 5, 542-545.	6.2	28
21	Colloidâ€Mediated Fabrication of a 3D Pollen Sponge for Oil Remediation Applications. Advanced Functional Materials, 2021, 31, 2101091.	7.8	28
22	Mechanistic Aspects of the Evolution of 3D Cholesterol Crystallites in a Supported Lipid Membrane via a Quartz Crystal Microbalance with Dissipation Monitoring. Langmuir, 2021, 37, 4562-4570.	1.6	2
23	Graphene Oxide Mimics Biological Signaling Cue to Rescue Starving Bacteria. Advanced Functional Materials, 2021, 31, 2102328.	7.8	3
24	An Intrinsically Microâ€∤Nanostructured Pollen Substrate with Tunable Optical Properties for Optoelectronic Applications. Advanced Materials, 2021, 33, e2100566.	11.1	9
25	Ultrahigh surface sensitivity of deposited gold nanorod arrays for nanoplasmonic biosensing. Applied Materials Today, 2021, 23, 101046.	2.3	6
26	3D Pollen Sponge: Colloidâ€Mediated Fabrication of a 3D Pollen Sponge for Oil Remediation Applications (Adv. Funct. Mater. 24/2021). Advanced Functional Materials, 2021, 31, 2170173.	7.8	2
27	Unraveling How Multivalency Triggers Shape Deformation of Sub-100 nm Lipid Vesicles. Journal of Physical Chemistry Letters, 2021, 12, 6722-6729.	2.1	11
28	Entrepreneurial Talent Building for 21st Century Agricultural Innovation. ACS Nano, 2021, 15, 10748-10758.	7.3	17
29	Solvent-induced conformational tuning of lysozyme protein adlayers on silica surfaces: A QCM-D and LSPR study. International Journal of Biological Macromolecules, 2021, 182, 1906-1914.	3.6	6
30	Engineering Natural Pollen Grains as Multifunctional 3D Printing Materials. Advanced Functional Materials, 2021, 31, 2106276.	7.8	15
31	Biophysical Measurement Strategies for Antiviral Drug Development: Recent Progress in Virus-Mimetic Platforms Down to the Single Particle Level. Accounts of Chemical Research, 2021, 54, 3204-3214.	7.6	3
32	Dynamic remodeling of giant unilamellar vesicles induced by monoglyceride nano-micelles: Insights into supramolecular organization. Applied Materials Today, 2021, 24, 101099.	2.3	5
33	Lipid bilayer coatings for rapid enzyme-linked immunosorbent assay. Applied Materials Today, 2021, 24, 101128.	2.3	5
34	Lipid Nanoparticle Technology for Delivering Biologically Active Fatty Acids and Monoglycerides. International Journal of Molecular Sciences, 2021, 22, 9664.	1.8	18
35	Supported lipid bilayer coatings: Fabrication, bioconjugation, and diagnostic applications. Applied Materials Today, 2021, 25, 101183.	2.3	13
36	Digital printing of shape-morphing natural materials. Proceedings of the National Academy of Sciences of the United States of America, 2021, 118, .	3.3	21

NAM-JOON CHO

#	Article	IF	CITATIONS
37	Role of Membrane Stretch in Adsorption of Antiviral Peptides onto Lipid Membranes and Membrane Pore Formation. Langmuir, 2021, 37, 13390-13398.	1.6	8
38	Surface engineering of plasmonic gold nanoisland platforms for high-sensitivity refractometric biosensing applications. Applied Materials Today, 2021, 26, 101280.	2.3	4
39	Engineering Natural Pollen Grains as Multifunctional 3D Printing Materials (Adv. Funct. Mater.) Tj ETQq1 1 0.7	84314 rgBT 7.8	/Overlock 10
40	Disentangling bulk polymers from adsorbed polymers using the quartz crystal microbalance. Applied Materials Today, 2020, 18, 100460.	2.3	3
41	Probing the influence of tether density on tethered bilayer lipid membrane (tBLM)-peptide interactions. Applied Materials Today, 2020, 18, 100527.	2.3	5
42	Hydrophobic to superhydrophilic tuning of multifunctional sporopollenin for microcapsule and bio-composite applications. Applied Materials Today, 2020, 18, 100525.	2.3	12
43	Optimal formation of uniform-phase supported lipid bilayers from phospholipid–monoglyceride bicellar mixtures. Journal of Industrial and Engineering Chemistry, 2020, 88, 285-291.	2.9	9
44	Unraveling How Ethanol-Induced Conformational Changes Affect BSA Protein Adsorption onto Silica Surfaces. Langmuir, 2020, 36, 9215-9224.	1.6	14
45	Medicinal Activities and Nanomedicine Delivery Strategies for Brucea javanica Oil and Its Molecular Components. Molecules, 2020, 25, 5414.	1.7	12
46	Conformational flexibility of fatty acid-free bovine serum albumin proteins enables superior antifouling coatings. Communications Materials, 2020, 1, .	2.9	44
47	Lipid-Bicelle-Coated Microfluidics for Intracellular Delivery with Reduced Fouling. ACS Applied Materials & amp; Interfaces, 2020, 12, 45744-45752.	4.0	15
48	Cloaking Silica Nanoparticles with Functional Protein Coatings for Reduced Complement Activation and Cellular Uptake. ACS Nano, 2020, 14, 11950-11961.	7.3	39
49	Elucidating How Different Amphipathic Stabilizers Affect BSA Protein Conformational Properties and Adsorption Behavior. Langmuir, 2020, 36, 10606-10614.	1.6	13
50	Versatile formation of supported lipid bilayers from bicellar mixtures of phospholipids and capric acid. Scientific Reports, 2020, 10, 13849.	1.6	11
51	Crystallization of Cholesterol in Phospholipid Membranes Follows Ostwald's Rule of Stages. Journal of the American Chemical Society, 2020, 142, 21872-21882.	6.6	14
52	Materials science approaches in the development of broad-spectrum antiviral therapies. Nature Materials, 2020, 19, 813-816.	13.3	36
53	pH-Dependent Antibacterial Activity of Glycolic Acid: Implications for Anti-Acne Formulations. Scientific Reports, 2020, 10, 7491.	1.6	13
54	Competing Interactions of Fatty Acids and Monoglycerides Trigger Synergistic Phospholipid Membrane Remodeling. Journal of Physical Chemistry Letters, 2020, 11, 4951-4957.	2.1	22

#	Article	IF	CITATIONS
55	Understanding how natural sequence variation in serum albumin proteins affects conformational stability and protein adsorption. Colloids and Surfaces B: Biointerfaces, 2020, 194, 111194.	2.5	17
56	Unraveling how nanoscale curvature drives formation of lysozyme protein monolayers on inorganic oxide surfaces. Applied Materials Today, 2020, 20, 100729.	2.3	2
57	Transformation of hard pollen into soft matter. Nature Communications, 2020, 11, 1449.	5.8	58
58	Microrobots Derived from Variety Plant Pollen Grains for Efficient Environmental Clean Up and as an Anti ancer Drug Carrier. Advanced Functional Materials, 2020, 30, 2000112.	7.8	64
59	Biologically interfaced nanoplasmonic sensors. Nanoscale Advances, 2020, 2, 3103-3114.	2.2	10
60	Influence of Chemical and Physical Change of Pollen Microgels on Swelling/Deâ€&welling Behavior. Macromolecular Rapid Communications, 2020, 41, e2000155.	2.0	9
61	A facile approach to patterning pollen microparticles for in situ imaging. Applied Materials Today, 2020, 20, 100702.	2.3	2
62	Scalable Fabrication of Quasi-One-Dimensional Gold Nanoribbons for Plasmonic Sensing. Nano Letters, 2020, 20, 1747-1754.	4.5	19
63	Degradation of the sporopollenin exine capsules (SECs) in human plasma. Applied Materials Today, 2020, 19, 100594.	2.3	7
64	Supported lipid bilayer platform for characterizing the optimization of mixed monoglyceride nano-micelles. Applied Materials Today, 2020, 19, 100598.	2.3	7
65	Lipid Bicelle Micropatterning Using Chemical Lift-Off Lithography. ACS Applied Materials & Interfaces, 2020, 12, 13447-13455.	4.0	13
66	Photocurable Albumin Methacryloyl Hydrogels as a Versatile Platform for Tissue Engineering. ACS Applied Bio Materials, 2020, 3, 920-934.	2.3	33
67	Supported Lipid Bilayer Formation: Beyond Vesicle Fusion. Langmuir, 2020, 36, 1387-1400.	1.6	94
68	Actuation and locomotion driven by moisture in paper made with natural pollen. Proceedings of the National Academy of Sciences of the United States of America, 2020, 117, 8711-8718.	3.3	68
69	Supported Lipid Bilayer Formation from Phospholipid-Fatty Acid Bicellar Mixtures. Langmuir, 2020, 36, 5021-5029.	1.6	14
70	Species-Specific Biodegradation of Sporopollenin-Based Microcapsules. Scientific Reports, 2019, 9, 9626.	1.6	14
71	Molecular diffusion and nano-mechanical properties of multi-phase supported lipid bilayers. Physical Chemistry Chemical Physics, 2019, 21, 16686-16693.	1.3	20
72	Comparing the Membrane-Interaction Profiles of Two Antiviral Peptides: Insights into Structure–Function Relationship. Langmuir, 2019, 35, 9934-9943.	1.6	25

#	Article	IF	CITATIONS
73	Influence of NaCl Concentration on Bicelle-Mediated SLB Formation. Langmuir, 2019, 35, 10658-10666.	1.6	25
74	Quantitative accounting of dye leakage and photobleaching in single lipid vesicle measurements: Implications for biomacromolecular interaction analysis. Colloids and Surfaces B: Biointerfaces, 2019, 182, 110338.	2.5	5
75	Porcine hepatocytes culture on biofunctionalized 3D inverted colloidal crystal scaffolds as an <i>in vitro</i> model for predicting drug hepatotoxicity. RSC Advances, 2019, 9, 17995-18007.	1.7	7
76	Characterizing the Supported Lipid Membrane Formation from Cholesterol-Rich Bicelles. Langmuir, 2019, 35, 15063-15070.	1.6	26
77	Surface-Based Nanoplasmonic Sensors for Biointerfacial Science Applications. Bulletin of the Chemical Society of Japan, 2019, 92, 1404-1412.	2.0	40
78	Dynamic Control of Intramolecular Rotation by Tuning the Surrounding Two-Dimensional Matrix Field. ACS Nano, 2019, 13, 2410-2419.	7.3	34
79	Solvent-assisted preparation of supported lipid bilayers. Nature Protocols, 2019, 14, 2091-2118.	5.5	70
80	In-depth characterization of congenital Zika syndrome in immunocompetent mice: Antibody-dependent enhancement and an antiviral peptide therapy. EBioMedicine, 2019, 44, 516-529.	2.7	27
81	Understanding How Membrane Surface Charge Influences Lipid Bicelle Adsorption onto Oxide Surfaces. Langmuir, 2019, 35, 8436-8444.	1.6	18
82	Improved Size Determination by Nanoparticle Tracking Analysis: Influence of Recognition Radius. Analytical Chemistry, 2019, 91, 9508-9515.	3.2	15
83	Modulating conformational stability of human serum albumin and implications for surface passivation applications. Colloids and Surfaces B: Biointerfaces, 2019, 180, 306-312.	2.5	11
84	Gelatin methacryloyl and its hydrogels with an exceptional degree of controllability and batch-to-batch consistency. Scientific Reports, 2019, 9, 6863.	1.6	204
85	Response of microbial membranes to butanol: interdigitationvs.disorder. Physical Chemistry Chemical Physics, 2019, 21, 11903-11915.	1.3	19
86	Microfluidic liquid cell chamber for scanning probe microscopy measurement application. Review of Scientific Instruments, 2019, 90, 046105.	0.6	10
87	Validation of Size Estimation of Nanoparticle Tracking Analysis on Polydisperse Macromolecule Assembly. Scientific Reports, 2019, 9, 2639.	1.6	88
88	Minimal Reconstitution of Membranous Web Induced by a Vesicle–Peptide Sol–Gel Transition. Biomacromolecules, 2019, 20, 1709-1718.	2.6	4
89	Human blood plasma catalyses the degradation of Lycopodium plant sporoderm microcapsules. Scientific Reports, 2019, 9, 2944.	1.6	7
90	Micropatterned Viral Membrane Clusters for Antiviral Drug Evaluation. ACS Applied Materials & Interfaces, 2019, 11, 13984-13990.	4.0	7

#	Article	IF	CITATIONS
91	Nanoplasmonic Sensor Detects Preferential Binding of IRSp53 to Negative Membrane Curvature. Frontiers in Chemistry, 2019, 7, 1.	1.8	439
92	Characterizing the Membrane-Disruptive Behavior of Dodecylglycerol Using Supported Lipid Bilayers. Langmuir, 2019, 35, 3568-3575.	1.6	14
93	Nanoarchitectonicâ€Based Material Platforms for Environmental and Bioprocessing Applications. Chemical Record, 2019, 19, 1891-1912.	2.9	17
94	Targeting the Achilles Heel of Mosquito-Borne Viruses for Antiviral Therapy. ACS Infectious Diseases, 2019, 5, 4-8.	1.8	24
95	Hybrid Biomimetic Interfaces Integrating Supported Lipid Bilayers with Decellularized Extracellular Matrix Components. Langmuir, 2018, 34, 3507-3516.	1.6	10
96	Lightâ€Induced Surface Modification of Natural Plant Microparticles: Toward Colloidal Science and Cellular Adhesion Applications. Advanced Functional Materials, 2018, 28, 1707568.	7.8	20
97	Preserving the inflated structure of lyophilized sporopollenin exine capsules with polyethylene glycol osmolyte. Journal of Industrial and Engineering Chemistry, 2018, 61, 255-264.	2.9	14
98	Interfacial Forces Dictate the Pathway of Phospholipid Vesicle Adsorption onto Silicon Dioxide Surfaces. Langmuir, 2018, 34, 1775-1782.	1.6	49
99	Effect of Glucose on the Mobility of Membrane-Adhering Liposomes. Langmuir, 2018, 34, 503-511.	1.6	4
100	Functionalized Natural Particles: Lightâ€Induced Surface Modification of Natural Plant Microparticles: Toward Colloidal Science and Cellular Adhesion Applications (Adv. Funct. Mater. 18/2018). Advanced Functional Materials, 2018, 28, 1870120.	7.8	0
101	Extraction of cage-like sporopollenin exine capsules from dandelion pollen grains. Scientific Reports, 2018, 8, 6565.	1.6	28
102	Complement activation in vitro and reactogenicity of low-molecular weight dextran-coated SPIONs in the pig CARPA model: Correlation with physicochemical features and clinical information. Journal of Controlled Release, 2018, 270, 268-274.	4.8	36
103	Nanoplasmonic sensors for detecting circulating cancer biomarkers. Advanced Drug Delivery Reviews, 2018, 125, 48-77.	6.6	88
104	A Numerical Study on the Effect of Particle Surface Coverage on the Quartz Crystal Microbalance Response. Analytical Chemistry, 2018, 90, 2238-2245.	3.2	28
105	Nanoplasmonic Ruler for Measuring Separation Distance between Supported Lipid Bilayers and Oxide Surfaces. Analytical Chemistry, 2018, 90, 12503-12511.	3.2	16
106	Characterizing How Acidic pH Conditions Affect the Membrane-Disruptive Activities of Lauric Acid and Glycerol Monolaurate. Langmuir, 2018, 34, 13745-13753.	1.6	27
107	Therapeutic treatment of Zika virus infection using a brain-penetrating antiviral peptide. Nature Materials, 2018, 17, 971-977.	13.3	74
108	Temperature-Induced Denaturation of BSA Protein Molecules for Improved Surface Passivation Coatings. ACS Applied Materials & amp; Interfaces, 2018, 10, 32047-32057.	4.0	77

#	Article	IF	CITATIONS
109	Nanoplasmonic Sensing Architectures for Decoding Membrane Curvature-Dependent Biomacromolecular Interactions. Analytical Chemistry, 2018, 90, 7458-7466.	3.2	16
110	Fluorescence-based immunosensor using three-dimensional CNT network structure for sensitive and reproducible detection of oral squamous cell carcinoma biomarker. Analytica Chimica Acta, 2018, 1027, 101-108.	2.6	34
111	Materials Nanoarchitectonics for Mechanical Tools in Chemical and Biological Sensing. Chemistry - an Asian Journal, 2018, 13, 3366-3377.	1.7	40
112	Membrane Reconstitution of Monoamine Oxidase Enzymes on Supported Lipid Bilayers. Langmuir, 2018, 34, 10764-10773.	1.6	4
113	Macromolecular Microencapsulation Using Pine Pollen: Loading Optimization and Controlled Release with Natural Materials. ACS Applied Materials & amp; Interfaces, 2018, 10, 28428-28439.	4.0	24
114	Fabrication of Multicomponent, Spatially Segregated DNA and Protein-Functionalized Supported Membrane Microarray. Langmuir, 2018, 34, 9781-9788.	1.6	10
115	Spatially Controlled Molecular Encapsulation in Natural Pine Pollen Microcapsules. Particle and Particle Systems Characterization, 2018, 35, 1800151.	1.2	8
116	Human iPS derived progenitors bioengineered into liver organoids using an inverted colloidal crystal poly (ethylene glycol) scaffold. Biomaterials, 2018, 182, 299-311.	5.7	93
117	Antibacterial Free Fatty Acids and Monoglycerides: Biological Activities, Experimental Testing, and Therapeutic Applications. International Journal of Molecular Sciences, 2018, 19, 1114.	1.8	325
118	Quantitative Comparison of Protein Adsorption and Conformational Changes on Dielectric-Coated Nanoplasmonic Sensing Arrays. Sensors, 2018, 18, 1283.	2.1	19
119	Membrane adaptation limitations in <i>Enterococcus faecalis</i> underlie sensitivity and the inability to develop significant resistance to conjugated oligoelectrolytes. RSC Advances, 2018, 8, 10284-10293.	1.7	15
120	Amyloid-β Peptide Triggers Membrane Remodeling in Supported Lipid Bilayers Depending on Their Hydrophobic Thickness. Langmuir, 2018, 34, 9548-9560.	1.6	18
121	Targeting the Achilles Heel of Zika Virus and Other Emerging Viral Pathogens. Advanced Therapeutics, 2018, 1, 1800045.	1.6	3
122	Hydrolytic Stability of Methacrylamide and Methacrylate in Gelatin Methacryloyl and Decoupling of Gelatin Methacrylamide from Gelatin Methacryloyl through Hydrolysis. Macromolecular Chemistry and Physics, 2018, 219, 1800266.	1.1	26
123	Envisioning Scientific Innovation in Korea's Demilitarized Zone: A Step toward Economic Progress and Global Peace. ACS Nano, 2018, 12, 5073-5077.	7.3	1
124	Self-association and conformational variation of NS5A domain 1 of hepatitis C virus. Journal of General Virology, 2018, 99, 194-208.	1.3	2
125	A Broad-Spectrum Antiviral Peptide for Combating Emerging Viral Pathogens. Proceedings for Annual Meeting of the Japanese Pharmacological Society, 2018, WCP2018, SY28-1.	0.0	0
126	Correlating Membrane Morphological Responses with Micellar Aggregation Behavior of Capric Acid and Monocaprin. Langmuir, 2017, 33, 2750-2759.	1.6	47

#	Article	IF	CITATIONS
127	High-performance, flexible electronic skin sensor incorporating natural microcapsule actuators. Nano Energy, 2017, 36, 38-45.	8.2	160
128	A flexible, ultra-sensitive chemical sensor with 3D biomimetic templating for diabetes-related acetone detection. Journal of Materials Chemistry B, 2017, 5, 4019-4024.	2.9	76
129	Optimizing the Formation of Supported Lipid Bilayers from Bicellar Mixtures. Langmuir, 2017, 33, 5052-5064.	1.6	52
130	Plantâ€Based Hollow Microcapsules for Oral Delivery Applications: Toward Optimized Loading and Controlled Release. Advanced Functional Materials, 2017, 27, 1700270.	7.8	74
131	Chemical processing strategies to obtain sporopollenin exine capsules from multi-compartmental pine pollen. Journal of Industrial and Engineering Chemistry, 2017, 53, 375-385.	2.9	24
132	Co-assembly of Peptide Amphiphiles and Lipids into Supramolecular Nanostructures Driven by Anionâ^'Ï€ Interactions. Journal of the American Chemical Society, 2017, 139, 7823-7830.	6.6	75
133	Cell Adhesion: Dynamic Cellular Interactions with Extracellular Matrix Triggered by Biomechanical Tuning of Lowâ€Rigidity, Supported Lipid Membranes (Adv. Healthcare Mater. 10/2017). Advanced Healthcare Materials, 2017, 6, .	3.9	1
134	Probing Spatial Proximity of Supported Lipid Bilayers to Silica Surfaces by Localized Surface Plasmon Resonance Sensing. Analytical Chemistry, 2017, 89, 4301-4308.	3.2	22
135	Nanoplasmonic sensors for biointerfacial science. Chemical Society Reviews, 2017, 46, 3615-3660.	18.7	195
136	Dynamic Cellular Interactions with Extracellular Matrix Triggered by Biomechanical Tuning of Lowâ€Rigidity, Supported Lipid Membranes. Advanced Healthcare Materials, 2017, 6, 1700243.	3.9	21
137	Controlling adsorption and passivation properties of bovine serum albumin on silica surfaces by ionic strength modulation and cross-linking. Physical Chemistry Chemical Physics, 2017, 19, 8854-8865.	1.3	49
138	Investigating how vesicle size influences vesicle adsorption on titanium oxide: a competition between steric packing and shape deformation. Physical Chemistry Chemical Physics, 2017, 19, 2131-2139.	1.3	31
139	Quantitative Profiling of Nanoscale Liposome Deformation by a Localized Surface Plasmon Resonance Sensor. Analytical Chemistry, 2017, 89, 1102-1109.	3.2	52
140	Detection of Amphipathic Viral Peptide on Screen-Printed Electrodes by Liposome Rupture Impact Voltammetry. Analytical Chemistry, 2017, 89, 11753-11757.	3.2	7
141	Quantitative Evaluation of Viral Protein Binding to Phosphoinositide Receptors and Pharmacological Inhibition. Analytical Chemistry, 2017, 89, 9742-9750.	3.2	7
142	Bioinspired Spiky Micromotors Based on Sporopollenin Exine Capsules. Advanced Functional Materials, 2017, 27, 1702338.	7.8	92
143	Colloidal templating of highly ordered gelatin methacryloyl-based hydrogel platforms for three-dimensional tissue analogues. NPG Asia Materials, 2017, 9, e412-e412.	3.8	42
144	A model derived from hydrodynamic simulations for extracting the size of spherical particles from the quartz crystal microbalance. Analyst, The, 2017, 142, 3370-3379.	1.7	26

#	Article	IF	CITATIONS
145	Drug Delivery: Plantâ€Based Hollow Microcapsules for Oral Delivery Applications: Toward Optimized Loading and Controlled Release (Adv. Funct. Mater. 31/2017). Advanced Functional Materials, 2017, 27, .	7.8	Ο
146	Quartz Crystal Microbalance Model for Quantitatively Probing the Deformation of Adsorbed Particles at Low Surface Coverage. Analytical Chemistry, 2017, 89, 11711-11718.	3.2	26
147	Understanding How Sterols Regulate Membrane Remodeling in Supported Lipid Bilayers. Langmuir, 2017, 33, 14756-14765.	1.6	30
148	Indirect Nanoplasmonic Sensing Platform for Monitoring Temperature-Dependent Protein Adsorption. Analytical Chemistry, 2017, 89, 12976-12983.	3.2	36
149	Influence of natural organic matter (NOM) coatings on nanoparticle adsorption onto supported lipid bilayers. Journal of Hazardous Materials, 2017, 339, 264-273.	6.5	10
150	Immobilization Strategies for Functional Complement Convertase Assembly at Lipid Membrane Interfaces. Langmuir, 2017, 33, 7332-7342.	1.6	11
151	Mechanical properties of paraformaldehyde-treated individual cells investigated by atomic force microscopy and scanning ion conductance microscopy. Nano Convergence, 2017, 4, 5.	6.3	72
152	Probing the Interaction of Dielectric Nanoparticles with Supported Lipid Membrane Coatings on Nanoplasmonic Arrays. Sensors, 2017, 17, 1484.	2.1	16
153	Optimizing the Performance of Supported Lipid Bilayers as Cell Culture Platforms Based on Extracellular Matrix Functionalization. ACS Omega, 2017, 2, 2395-2404.	1.6	23
154	Long-term culture of human liver tissue with advanced hepatic functions. JCI Insight, 2017, 2, .	2.3	23
155	Nanotechnology Formulations for Antibacterial Free Fatty Acids and Monoglycerides. Molecules, 2016, 21, 305.	1.7	88
156	Natural Products for the Treatment of Chlamydiaceae Infections. Microorganisms, 2016, 4, 39.	1.6	20
157	Spheroid Formation of Hepatocarcinoma Cells in Microwells: Experiments and Monte Carlo Simulations. PLoS ONE, 2016, 11, e0161915.	1.1	21
158	Preparation of Highly Monodisperse Electroactive Pollen Biocomposites. ChemNanoMat, 2016, 2, 414-418.	1.5	6
159	Plasmonic Nanohole Sensor for Capturing Single Virusâ€Like Particles toward Virucidal Drug Evaluation. Small, 2016, 12, 1159-1166.	5.2	57
160	Nanomedicine for Infectious Disease Applications: Innovation towards Broadâ€ S pectrum Treatment of Viral Infections. Small, 2016, 12, 1133-1139.	5.2	52
161	Natural Sunflower Pollen as a Drug Delivery Vehicle. Small, 2016, 12, 1167-1173.	5.2	81
162	Biofunctionalized Hydrogel Microscaffolds Promote 3D Hepatic Sheet Morphology. Macromolecular Bioscience, 2016, 16, 314-321.	2.1	19

#	Article	IF	CITATIONS
163	<i>Lycopodium</i> Spores: A Naturally Manufactured, Superrobust Biomaterial for Drug Delivery. Advanced Functional Materials, 2016, 26, 487-497.	7.8	47
164	Grapheneâ€Functionalized Natural Microcapsules: Modular Building Blocks for Ultrahigh Sensitivity Bioelectronic Platforms. Advanced Functional Materials, 2016, 26, 2097-2103.	7.8	75
165	ECM proteins in a microporous scaffold influence hepatocyte morphology, function, and gene expression. Scientific Reports, 2016, 6, 37427.	1.6	29
166	Pulled microcapillary tube resonators with electrical readout for mass sensing applications. Scientific Reports, 2016, 6, 33799.	1.6	19
167	Biosensors: Flexible, Graphene-Coated Biocomposite for Highly Sensitive, Real-Time Molecular Detection (Adv. Funct. Mater. 47/2016). Advanced Functional Materials, 2016, 26, 8796-8796.	7.8	Ο
168	Eco-friendly streamlined process for sporopollenin exine capsule extraction. Scientific Reports, 2016, 6, 19960.	1.6	56
169	Particle Tracking: Probing Membrane Viscosity and Interleaflet Friction of Supported Lipid Bilayers by Tracking Electrostatically Adsorbed, Nano-Sized Vesicles (Small 46/2016). Small, 2016, 12, 6304-6304.	5.2	0
170	Envisioning the Future of Nanotechnology Platforms for Biomedicine. Small, 2016, 12, 1116-1116.	5.2	1
171	Brownian Dynamics of Electrostatically Adhering Small Vesicles to a Membrane Surface Induces Domains and Probes Viscosity. Langmuir, 2016, 32, 5445-5450.	1.6	8
172	Controlling the Formation of Phospholipid Monolayer, Bilayer, and Intact Vesicle Layer on Graphene. ACS Applied Materials & Interfaces, 2016, 8, 11875-11880.	4.0	37
173	Influence of Divalent Cations on Deformation and Rupture of Adsorbed Lipid Vesicles. Langmuir, 2016, 32, 6486-6495.	1.6	56
174	Improving Taxane-Based Chemotherapy in Castration-Resistant Prostate Cancer. Trends in Pharmacological Sciences, 2016, 37, 451-462.	4.0	45
175	Multistep Compositional Remodeling of Supported Lipid Membranes by Interfacially Active Phosphatidylinositol Kinases. Analytical Chemistry, 2016, 88, 5042-5045.	3.2	11
176	Correlating single-molecule and ensemble-average measurements of peptide adsorption onto different inorganic materials. Physical Chemistry Chemical Physics, 2016, 18, 14454-14459.	1.3	14
177	Hydrodynamic Propulsion of Liposomes Electrostatically Attracted to a Lipid Membrane Reveals Size-Dependent Conformational Changes. ACS Nano, 2016, 10, 8812-8820.	7.3	12
178	Kinetics of the formation of a protein corona around nanoparticles. Mathematical Biosciences, 2016, 282, 82-90.	0.9	39
179	Probing Membrane Viscosity and Interleaflet Friction of Supported Lipid Bilayers by Tracking Electrostatically Adsorbed, Nanoâ€ s ized Vesicles. Small, 2016, 12, 6338-6344.	5.2	10
180	Midbrain-like Organoids from Human Pluripotent Stem Cells Contain Functional Dopaminergic and Neuromelanin-Producing Neurons. Cell Stem Cell, 2016, 19, 248-257.	5.2	628

#	Article	IF	CITATIONS
181	A phenomenological model of the solvent-assisted lipid bilayer formation method. Physical Chemistry Chemical Physics, 2016, 18, 24157-24163.	1.3	19
182	Integration of Quartz Crystal Microbalance-Dissipation and Reflection-Mode Localized Surface Plasmon Resonance Sensors for Biomacromolecular Interaction Analysis. Analytical Chemistry, 2016, 88, 12524-12531.	3.2	46
183	Influence of membrane surface charge on adsorption of complement proteins onto supported lipid bilayers. Colloids and Surfaces B: Biointerfaces, 2016, 148, 270-277.	2.5	14
184	Flexible, Grapheneâ€Coated Biocomposite for Highly Sensitive, Realâ€Time Molecular Detection. Advanced Functional Materials, 2016, 26, 8623-8630.	7.8	116
185	Precise Tuning of Facile One-Pot Gelatin Methacryloyl (GelMA) Synthesis. Scientific Reports, 2016, 6, 31036.	1.6	270
186	Multifunctional hydrogel nano-probes for atomic force microscopy. Nature Communications, 2016, 7, 11566.	5.8	44
187	Inflated Sporopollenin Exine Capsules Obtained from Thin-Walled Pollen. Scientific Reports, 2016, 6, 28017.	1.6	25
188	Extracellular Matrix Functionalization and Huh-7.5 Cell Coculture Promote the Hepatic Differentiation of Human Adipose-Derived Mesenchymal Stem Cells in a 3D ICC Hydrogel Scaffold. ACS Biomaterials Science and Engineering, 2016, 2, 2255-2265.	2.6	13
189	High-performance 3D printing of hydrogels by water-dispersible photoinitiator nanoparticles. Science Advances, 2016, 2, e1501381.	4.7	191
190	Stealth Immune Properties of Graphene Oxide Enabled by Surface-Bound Complement Factor H. ACS Nano, 2016, 10, 10161-10172.	7.3	49
191	Extraction of Plant-based Capsules for Microencapsulation Applications. Journal of Visualized Experiments, 2016, , .	0.2	3
192	Fabrication of Inverted Colloidal Crystal Poly(ethylene glycol) Scaffold: A Three-dimensional Cell Culture Platform for Liver Tissue Engineering. Journal of Visualized Experiments, 2016, , .	0.2	10
193	Nanotechnology Education for the Global World: Training the Leaders of Tomorrow. ACS Nano, 2016, 10, 5595-5599.	7.3	43
194	Reconstitution and Functional Analysis of a Full-Length Hepatitis C Virus NS5B Polymerase on a Supported Lipid Bilayer. ACS Central Science, 2016, 2, 456-466.	5.3	7
195	Extraction of sporopollenin exine capsules from sunflower pollen grains. RSC Advances, 2016, 6, 16533-16539.	1.7	55
196	Size-dependent, stochastic nature of lipid exchange between nano-vesicles and model membranes. Nanoscale, 2016, 8, 13513-13520.	2.8	9
197	Biosensors: Graphene-Functionalized Natural Microcapsules: Modular Building Blocks for Ultrahigh Sensitivity Bioelectronic Platforms (Adv. Funct. Mater. 13/2016). Advanced Functional Materials, 2016, 26, 2220-2220.	7.8	1
198	Supported lipid bilayer repair mediated by AH peptide. Physical Chemistry Chemical Physics, 2016, 18, 3040-3047.	1.3	14

#	Article	IF	CITATIONS
199	Phenotypic regulation of liver cells in a biofunctionalized three-dimensional hydrogel platform. Integrative Biology (United Kingdom), 2016, 8, 156-166.	0.6	14
200	Comparison of complement activation-related pseudoallergy in miniature and domestic pigs: foundation of a validatable immune toxicity model. Nanomedicine: Nanotechnology, Biology, and Medicine, 2016, 12, 933-943.	1.7	55
201	Deciphering How Pore Formation Causes Strain-Induced Membrane Lysis of Lipid Vesicles. Journal of the American Chemical Society, 2016, 138, 1406-1413.	6.6	40
202	Drug Delivery: <i>Lycopodium</i> Spores: A Naturally Manufactured, Superrobust Biomaterial for Drug Delivery (Adv. Funct. Mater. 4/2016). Advanced Functional Materials, 2016, 26, 632-632.	7.8	1
203	Encapsulation and controlled release formulations of 5-fluorouracil from natural Lycopodium clavatum spores. Journal of Industrial and Engineering Chemistry, 2016, 36, 102-108.	2.9	49
204	Self-assembly and sequence length dependence on nanofibrils of polyglutamine peptides. Neuropeptides, 2016, 57, 71-83.	0.9	4
205	Relationship between vesicle size and steric hindrance influences vesicle rupture on solid supports. Physical Chemistry Chemical Physics, 2016, 18, 3065-3072.	1.3	19
206	Nanoplasmonic ruler to measure lipid vesicle deformation. Chemical Communications, 2016, 52, 76-79.	2.2	46
207	Cholesterol-Enriched Domain Formation Induced by Viral-Encoded, Membrane-Active Amphipathic Peptide. Biophysical Journal, 2016, 110, 176-187.	0.2	20
208	Antiviral Agents: Correlation between Membrane Partitioning and Functional Activity in a Single Lipid Vesicle Assay Establishes Design Guidelines for Antiviral Peptides (Small 20/2015). Small, 2015, 11, 2464-2464.	5.2	0
209	Biomembrane Fabrication by the Solvent-assisted Lipid Bilayer (SALB) Method. Journal of Visualized Experiments, 2015, , .	0.2	15
210	"Multipoint Force Feedback―Leveling of Massively Parallel Tip Arrays in Scanning Probe Lithography. Small, 2015, 11, 4526-4531.	5.2	11
211	Natural Products for the Treatment of Trachoma and Chlamydia trachomatis. Molecules, 2015, 20, 4180-4203.	1.7	25
212	Modulation of Huh7.5 Spheroid Formation and Functionality Using Modified PEG-Based Hydrogels of Different Stiffness. PLoS ONE, 2015, 10, e0118123.	1.1	47
213	Membrane attack complex formation on a supported lipid bilayer: initial steps towards a CARPA predictor nanodevice. European Journal of Nanomedicine, 2015, 7, .	0.6	8
214	Efficient and controllable synthesis of highly substituted gelatin methacrylamide for mechanically stiff hydrogels. RSC Advances, 2015, 5, 106094-106097.	1.7	118
215	Spatiotemporal dynamics of solvent-assisted lipid bilayer formation. Physical Chemistry Chemical Physics, 2015, 17, 31145-31151.	1.3	11
216	Solvent-Assisted Lipid Self-Assembly at Hydrophilic Surfaces: Factors Influencing the Formation of Supported Membranes. Langmuir, 2015, 31, 3125-3134.	1.6	66

#	Article	IF	CITATIONS
217	Contribution of Temperature to Deformation of Adsorbed Vesicles Studied by Nanoplasmonic Biosensing. Langmuir, 2015, 31, 771-781.	1.6	44
218	Self-Assembly Formation of Lipid Bilayer Coatings on Bare Aluminum Oxide: Overcoming the Force of Interfacial Water. ACS Applied Materials & Interfaces, 2015, 7, 959-968.	4.0	68
219	Correlation between Membrane Partitioning and Functional Activity in a Single Lipid Vesicle Assay Establishes Design Guidelines for Antiviral Peptides. Small, 2015, 11, 2372-2379.	5.2	30
220	Alternative configuration scheme for signal amplification with scanning ion conductance microscopy. Review of Scientific Instruments, 2015, 86, 023706.	0.6	8
221	Influence of pH and Surface Chemistry on Poly(<scp>l</scp> -lysine) Adsorption onto Solid Supports Investigated by Quartz Crystal Microbalance with Dissipation Monitoring. Journal of Physical Chemistry B, 2015, 119, 10554-10565.	1.2	43
222	Quantitative Evaluation of Peptide–Material Interactions by a Force Mapping Method: Guidelines for Surface Modification. Langmuir, 2015, 31, 8006-8012.	1.6	14
223	Elucidating how bamboo salt interacts with supported lipid membranes: influence of alkalinity on membrane fluidity. European Biophysics Journal, 2015, 44, 383-391.	1.2	0
224	Peptide-induced formation of a tethered lipid bilayer membrane on mesoporous silica. European Biophysics Journal, 2015, 44, 27-36.	1.2	18
225	Adsorption of hyaluronic acid on solid supports: Role of pH and surface chemistry in thin film self-assembly. Journal of Colloid and Interface Science, 2015, 448, 197-207.	5.0	25
226	Fabrication of charged membranes by the solvent-assisted lipid bilayer (SALB) formation method on SiO ₂ and Al ₂ O ₃ . Physical Chemistry Chemical Physics, 2015, 17, 11546-11552.	1.3	30
227	Strategies for enhancing the sensitivity of plasmonic nanosensors. Nano Today, 2015, 10, 213-239.	6.2	356
228	Supported Lipid Bilayer Platform To Test Inhibitors of the Membrane Attack Complex: Insights into Biomacromolecular Assembly and Regulation. Biomacromolecules, 2015, 16, 3594-3602.	2.6	18
229	Spectrum of Membrane Morphological Responses to Antibacterial Fatty Acids and Related Surfactants. Langmuir, 2015, 31, 10223-10232.	1.6	80
230	Phosphatidylinositol 4,5-Bisphosphate Is an HCV NS5A Ligand and Mediates Replication of the Viral Genome. Gastroenterology, 2015, 148, 616-625.	0.6	37
231	Silk fibroin–keratin based 3D scaffolds as a dermal substitute for skin tissue engineering. Integrative Biology (United Kingdom), 2015, 7, 53-63.	0.6	139
232	Effect of a Non-Newtonian Load on SignatureS2for Quartz Crystal Microbalance Measurements. Journal of Sensors, 2014, 2014, 1-8.	0.6	3
233	Rupture of zwitterionic lipid vesicles by an amphipathic, α-helical peptide: Indirect effects of sensor surface and implications for experimental analysis. Colloids and Surfaces B: Biointerfaces, 2014, 121, 340-346.	2.5	15
234	Observation of Stripe Superstructure in the β-Two-Phase Coexistence Region of Cholesterol–Phospholipid Mixtures in Supported Membranes. Journal of the American Chemical Society, 2014, 136, 16962-16965.	6.6	27

#	Article	IF	CITATIONS
235	Biosensors: Controlling Lipid Membrane Architecture for Tunable Nanoplasmonic Biosensing (Small) Tj ETQq1 1	0.784314	ŀrg₽T /Overl⊂
236	Controlling Lipid Membrane Architecture for Tunable Nanoplasmonic Biosensing. Small, 2014, 10, 4828-4832.	5.2	42
237	Formation of Cholesterol-Rich Supported Membranes Using Solvent-Assisted Lipid Self-Assembly. Langmuir, 2014, 30, 13345-13352.	1.6	53
238	Solvent-Assisted Lipid Bilayer Formation on Silicon Dioxide and Gold. Langmuir, 2014, 30, 10363-10373.	1.6	134
239	Vesicle Adhesion and Rupture on Silicon Oxide: Influence of Freeze–Thaw Pretreatment. Langmuir, 2014, 30, 2152-2160.	1.6	47
240	AH Peptide-Mediated Formation of Charged Planar Lipid Bilayers. Journal of Physical Chemistry B, 2014, 118, 3616-3621.	1.2	33
241	Bimodal Tumor-Targeting from Microenvironment Responsive Hyaluronan Layer-by-Layer (LbL) Nanoparticles. ACS Nano, 2014, 8, 8374-8382.	7.3	161
242	Contribution of the Hydration Force to Vesicle Adhesion on Titanium Oxide. Langmuir, 2014, 30, 5368-5372.	1.6	52
243	Nanoplasmonic Biosensing for Soft Matter Adsorption: Kinetics of Lipid Vesicle Attachment and Shape Deformation. Langmuir, 2014, 30, 9494-9503.	1.6	54
244	Influence of Osmotic Pressure on Adhesion of Lipid Vesicles to Solid Supports. Langmuir, 2013, 29, 11375-11384.	1.6	81
245	Rupture of Lipid Vesicles by a Broad-Spectrum Antiviral Peptide: Influence of Vesicle Size. Journal of Physical Chemistry B, 2013, 117, 16117-16128.	1.2	56
246	Kinetics of the maintenance of the epidermis. Open Physics, 2013, 11, .	0.8	2
247	Comparison of Extruded and Sonicated Vesicles for Planar Bilayer Self-Assembly. Materials, 2013, 6, 3294-3308.	1.3	66
248	Biotechnology Applications of Tethered Lipid Bilayer Membranes. Materials, 2012, 5, 2637-2657.	1.3	101
249	BIOPHYSICAL APPLICATIONS OF SCANNING ION CONDUCTANCE MICROSCOPY (SICM). Modern Physics Letters B, 2012, 26, 1130003.	1.0	21
250	Single Vesicle Analysis Reveals Nanoscale Membrane Curvature Selective Pore Formation in Lipid Membranes by an Antiviral α-Helical Peptide. Nano Letters, 2012, 12, 5719-5725.	4.5	56
251	Chiral crystallization of aromatic helical foldamers via complementarities in shape and end functionalities. Chemical Science, 2012, 3, 2042.	3.7	52
252	Model Membrane Platforms for Biomedicine: Case Study on Antiviral Drug Development. Biointerphases, 2012, 7, 18.	0.6	39

#	Article	IF	CITATIONS
253	pH-Driven Assembly of Various Supported Lipid Platforms: A Comparative Study on Silicon Oxide and Titanium Oxide. Langmuir, 2011, 27, 3739-3748.	1.6	83
254	A small molecule inhibits HCV replication and alters NS4B's subcellular distribution. Antiviral Research, 2010, 87, 1-8.	1.9	42
255	Quartz crystal microbalance with dissipation monitoring of supported lipid bilayers on various substrates. Nature Protocols, 2010, 5, 1096-1106.	5.5	471
256	Identification of a Class of HCV Inhibitors Directed Against the Nonstructural Protein NS4B. Science Translational Medicine, 2010, 2, 15ra6.	5.8	52
257	Hydrophobic nanoparticles improve permeability of cell-encapsulating poly(ethylene glycol) hydrogels while maintaining patternability. Proceedings of the National Academy of Sciences of the United States of America, 2010, 107, 20709-20714.	3.3	34
258	Interfacial Binding Dynamics of Bee Venom Phospholipase A ₂ Investigated by Dynamic Light Scattering and Quartz Crystal Microbalance. Langmuir, 2010, 26, 4103-4112.	1.6	33
259	Fabrication of a Planar Zwitterionic Lipid Bilayer on Titanium Oxide. Langmuir, 2010, 26, 15706-15710.	1.6	49
260	Vesicle Adsorption on Mesoporous Silica and Titania. Langmuir, 2010, 26, 16630-16633.	1.6	28
261	Type I Collagen-Functionalized Supported Lipid Bilayer as a Cell Culture Platform. Biomacromolecules, 2010, 11, 1231-1240.	2.6	51
262	Analyzing Spur-Distorted Impedance Spectra for the QCM. Journal of Sensors, 2009, 2009, 1-8.	0.6	17
263	Quartz Crystal Microbalance as a Sensor to Characterize Macromolecular Assembly Dynamics. Journal of Sensors, 2009, 2009, 1-17.	0.6	50
264	Viral infection of human progenitor and liver-derived cells encapsulated in three-dimensional PEC-based hydrogel. Biomedical Materials (Bristol), 2009, 4, 011001.	1.7	30
265	The reliable targeting of specific drug release profiles by integrating arrays of different albumin-encapsulated microsphere types. Biomaterials, 2009, 30, 6648-6654.	5.7	10
266	Mechanism of an Amphipathic α-Helical Peptide's Antiviral Activity Involves Size-Dependent Virus Particle Lysis. ACS Chemical Biology, 2009, 4, 1061-1067.	1.6	71
267	Alpha-Helical Peptide-Induced Vesicle Rupture Revealing New Insight into the Vesicle Fusion Process As Monitored <i>in Situ</i> by Quartz Crystal Microbalance-Dissipation and Reflectometry. Analytical Chemistry, 2009, 81, 4752-4761.	3.2	45
268	Viral infection of human progenitor and liver-derived cells encapsulated in three-dimensional PEG-based hydrogel. Biomedical Materials (Bristol), 2009, 4, 011001.	1.7	18
269	Electrochemical-QCM Investigation of Solid-Supported Lipid Bilayer Formed by AH Peptide Derived from HCV's Nonstructural Protein. ECS Meeting Abstracts, 2008, , .	0.0	0
270	Binding Dynamics of Hepatitis C Virus' NS5A Amphipathic Peptide to Cell and Model Membranes. Journal of Virology, 2007, 81, 6682-6689.	1.5	38

Nam-Joon Cho

#	Article	IF	CITATIONS
271	Creation of Lipid Partitions by Deposition of Amphipathic Viral Peptides. Langmuir, 2007, 23, 10855-10863.	1.6	24
272	Employing an Amphipathic Viral Peptide to Create a Lipid Bilayer on Au and TiO ₂ . Journal of the American Chemical Society, 2007, 129, 10050-10051.	6.6	107
273	Quartz resonator signatures under Newtonian liquid loading for initial instrument check. Journal of Colloid and Interface Science, 2007, 315, 248-254.	5.0	40
274	Employing Two Different Quartz Crystal Microbalance Models To Study Changes in Viscoelastic Behavior upon Transformation of Lipid Vesicles to a Bilayer on a Gold Surface. Analytical Chemistry, 2007, 79, 7027-7035.	3.2	113